

Hollow Sodium Tungsten Bronze ($\text{Na}_{0.15}\text{WO}_3$) Nanospheres: Preparation, Characterization, and Their Adsorption Properties

Jing Hou · Guanke Zuo · Guangxia Shen ·
He Guo · Hui Liu · Ping Cheng ·
Jingyan Zhang · Shouwu Guo

Received: 23 April 2009 / Accepted: 1 July 2009 / Published online: 17 July 2009
© to the authors 2009

Abstract We report herein a facile method for the preparation of sodium tungsten bronzes hollow nanospheres using hydrogen gas bubbles as reactant for chemical reduction of tungstate to tungsten and as template for the formation of hollow nanospheres at the same time. The chemical composition and the crystalline state of the as-prepared hollow $\text{Na}_{0.15}\text{WO}_3$ nanospheres were characterized complementarily, and the hollow structure formation mechanism was proposed. The hollow $\text{Na}_{0.15}\text{WO}_3$ nanospheres showed large Brunauer–Emmett–Teller specific area ($33.8 \text{ m}^2 \text{ g}^{-1}$), strong resistance to acids, and excellent ability to remove organic molecules such as dye and proteins from aqueous solutions. These illustrate that the hollow nanospheres of $\text{Na}_{0.15}\text{WO}_3$ should be a useful adsorbent.

Keywords Sodium tungsten bronze ·
Hollow nanosphere · Adsorption property

Introduction

Hollow structure materials exhibit usually extraordinary adsorbing capacities to a wide range of species (i.e., metal ions, organic molecules, and biomolecules) and have found practical applications in catalysis [1, 2], water treatment [3], and drug delivery [4]. The hollow nanospheres, because of their unique physical and chemical properties, have attracted more significant interest during the last few years [5–9]. Up to now, several synthetic strategies have been developed, and a range of hollow nanospheres, especially metal oxides and sulfides, have been fabricated [3, 6, 8, 10–12], but it is still challenging to develop simple and reliable synthetic methods for hollow nanospheres with diverse chemical compositions, desired chemical/physical stabilities, and controlled size and shell structures (shell thickness and porosity), which are critical for their practical applications.

Sodium tungsten bronzes (Na_xWO_3 , $0 < x \leq 1$), besides their unique electronic/electric properties that vary greatly with their compositions [13–17], have inert chemical properties, such as insolubility in water and resistance to most acids except hydrofluoric [18], which make Na_xWO_3 promising for use in many extreme chemical cases. Nano-sized Na_xWO_3 , predictably, should have more enriched properties differing from that of the corresponding bulk materials and might find more novel applications, but have barely been explored [19]. We report herein a facile strategy for the fabrication of hollow nanospheres of sodium tungsten bronzes, Na_xWO_3 , and their potential applications in water treatment. The fabrication, including the control on sizes of

Electronic supplementary material The online version of this article (doi:10.1007/s11671-009-9383-x) contains supplementary material, which is available to authorized users.

J. Hou · G. Shen · P. Cheng · S. Guo (✉)
National Key Laboratory of Nano/Micro Fabrication Technology,
Key Laboratory for Thin Film and Microfabrication of the
Ministry of Education, Research Institute of Micro/Nano Science
and Technology, Shanghai Jiao Tong University,
200240 Shanghai, People's Republic of China
e-mail: swguo@sjtu.edu.cn

J. Hou
School of Materials Science & Engineering, East China
University of Science and Technology, 200237 Shanghai,
People's Republic of China

G. Zuo · H. Guo · H. Liu · J. Zhang (✉)
School of Pharmacy, East China University of Science and
Technology, 200237 Shanghai, People's Republic of China
e-mail: jyzhang@ecust.edu.cn

the spheres and hollow feature of the hollow Na_xWO_3 nanospheres, was achieved through reduction of aqueous sodium tungstate (Na_2WO_4) solution by sodium borohydride (NaBH_4) powder under well-controlled pH and temperature. The chemical composition, crystalline state, size, and morphology of the as-prepared hollow Na_xWO_3 nanospheres were characterized complementarily using scanning electron microscopy (SEM), transmission electron microscopy (TEM, including HRTEM), energy dispersive spectrum (EDS), X-ray photoelectron spectroscopy (XPS), and X-ray powder diffraction (XRD). Their application in the removal of organic molecules from water was illustrated using different molecules, such as Coomassie brilliant blue, Albumin Bovine, and Lysozyme.

Experimental

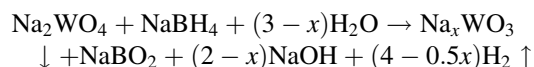
Sodium tungstate, sodium borohydride, hydrochloric acid (37%), and ethanol were purchased from Sinopharm Chemical Reagent Co., Ltd. (Shanghai, China) and used as received. Coomassie Brilliant blue, Lysozyme, and Albumin Bovine were from Sino-American Biotechnology Co. (Shanghai, China). Pure water (electric resistance of $18.2 \text{ M}\Omega \text{ cm}^{-1}$) was produced through an HF Super NW water purification system (Heal Force Co. Shanghai, China). A typical procedure for the preparation of hollow $\text{Na}_{0.15}\text{WO}_3$ nanospheres is as follows: 40 mL of 0.25 M Na_2WO_4 aqueous solution was put in a 250 mL flask and the pH of the solution was adjusted to 6.8 using concentrated HCl (37%). Then, 0.025 mol of NaBH_4 powder was added gradually into the Na_2WO_4 solution, and the mixture was stirred at room temperature ($\sim 25^\circ\text{C}$) for 2 h. After the reaction, the brown precipitate was separated from the reaction system by centrifugation, washed three times with pure water and two times with ethanol, and finally dried at 80°C under a vacuum. Solid $\text{Na}_{0.15}\text{WO}_3$ nanospheres were prepared under almost the same conditions used above except that the reaction temperature was 100°C and that the NaBH_4 powders must be added step-by-step because the reaction at 100°C takes place vigorously.

Coomassie Brilliant Blue and the proteins adsorption experiments were carried out at room temperature. The $\text{Na}_{0.15}\text{WO}_3$ was first dispersed into water or buffer; the stock solutions of Coomassie Brilliant blue or proteins were then added to the $\text{Na}_{0.15}\text{WO}_3$ suspension and incubated on the shaker. UV–vis absorption spectra of Coomassie Brilliant blue and proteins in the supernatant were recorded at different time intervals to follow the adsorption process. The gel electrophoresis was run on a DYY-6C electrophoresis system (Liuyi Electrophoresis Co., Beijing, China). The standard 15% SDS polyacrylamide gel was used and was run under constant voltage of 50 mV.

Scanning electron microscopy images were acquired on a SIRION 200 field emission scanning electron microscope (FEI Company, USA). TEM images and energy dispersive spectra (EDS) were taken on a JSM-2010 transmission electron microscope (JEOL Ltd., Japan) operated at 200 kV. The powders of $\text{Na}_{0.15}\text{WO}_3$ nanospheres were first suspended in water and then transferred on to silicon substrates or copper TEM grids for the SEM and TEM measurements, respectively. XRD patterns were recorded on a D/MAX 2200/PC diffractometer (Rigaku Corporation, Japan) using Cu $K\alpha$ radiation, $\lambda = 1.54 \text{ \AA}$. XPS measurement was performed on an Axis Ultra DLD instrument (Kratos Analytical, UK) using a monochromatized Al ($K\alpha$) source. UV–vis absorption spectra were recorded on a UV-2550 spectrometer (Shimadzu Corporation, Japan). The Brunauer–Emment–Teller (BET) specific area was measured on ASAP 2010 M/C surface area and porosity analyzer (Micromeritics Instrument Corporation, USA) based on N_2 adsorption.

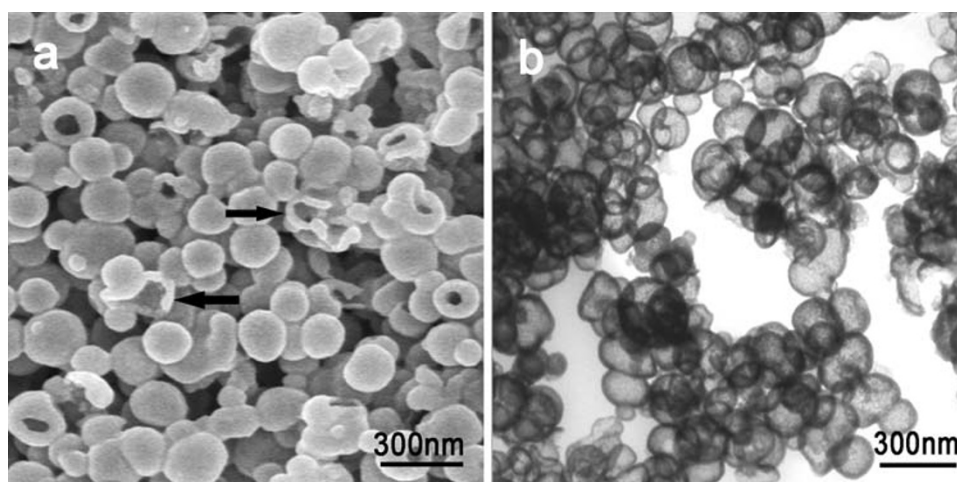
Results and Discussion

In general, the bulk sodium tungsten bronzes can be prepared through the following chemical reaction [20–23]:



In the reaction, the hydrogen generated from the hydrolysis of NaBH_4 under acidic reaction condition was partially consumed to reduce tungstate to tungsten, and the rest was released from the reaction system to the air [24]. Therefore, in practice, to prevent a rapid loss of hydrogen and to enhance the reduction ability of NaBH_4 , the aqueous solutions of Na_2WO_4 and NaBH_4 were mixed first, and the initial pH of mixture solution was maintained at 11 or above. The Na_2WO_4 reduction was initiated subsequently by adjusting the pH of the mixture down below 7 by adding acid, such as HCl. Thus, there were not too many hydrogen gas bubbles accumulated in the reaction system, the loss of the hydrogen gas could be suppressed, and powder of bulk sodium tungsten bronzes was obtained finally. In this work, instead of mixing two pre-prepared solutions, the reaction was conducted by adding the NaBH_4 powder directly into the Na_2WO_4 aqueous solutions. However, we found that when the pH of the Na_2WO_4 aqueous solution is above 10, the reaction took place very slow; under the acidic condition, $\text{pH} < 6$, the NaBH_4 was hydrolyzed rapidly and the as-generated hydrogen bubbles escaped from the reaction system severely. Hence, in a typical procedure of preparing Na_xWO_4 nanospheres in the work, Na_2WO_4 aqueous solutions with pH near to neutral (typically, 6.9–7.2) were prepared first, and NaBH_4 powder was then added gradually

Fig. 1 **a** FESEM image of hollow $\text{Na}_{0.15}\text{WO}_3$ nanospheres. The *arrows* indicate the broken hollow nanospheres from which the thickness, ~ 25 nm, of the shell of the hollow nanospheres was estimated. **b** TEM image of the hollow $\text{Na}_{0.15}\text{WO}_3$ nanospheres. The *dark edge* and *bright center* character of the TEM image of the nanospheres reveal the formation of the hollow structure



into the Na_2WO_4 solutions under moderate stirring at room temperature ($\sim 25^\circ\text{C}$). The total amount of NaBH_4 added was usually three times of Na_2WO_4 (molar ratio) to ensure the reduction of tungstate to tungsten. After completion of the reaction, the solid product was collected by centrifugation and was washed thoroughly using pure water and ethanol, and finally dried at 80°C under a vacuum (0.01 Torr).

Scanning electron microscopy image, in Fig. 1a, shows that the solid products are nanospheres with sizes ranging from a few 10 to 200 nm in diameter. As pointed out with arrows in Fig. 1a, some broken nanospheres have a vacant interior structure, and the shell thickness of the broken nanospheres is about 25 nm. This provides us with a hint that the as-obtained nanospheres might have a hollow structure. To confirm this assumption, the nanospheres were subjected to TEM measurement. As depicted in Fig. 1b, the TEM image of each nanosphere possesses the dark edge and bright center illustrating unambiguously their hollow nature. The averaged shell thickness of hollow spheres measured from the TEM images is ~ 25 nm. This is in full agreement with the data (~ 25 nm) measured on SEM images of the broken nanospheres (indicated via the dark arrows in Fig. 1a). In addition, on the SEM image (Fig. 1a), circular nano-holes (~ 20 – 40 nm in diameter) were observed on the shells of some nanospheres implying the formation of the open-shell hollow structures. It is impossible to take the images of the hollow nanospheres from all the directions at the same time, so the distribution of the nano-holes is unknown at the moment for us.

The chemical compositions and crystallinity of the as-synthesized hollow Na_xWO_3 nanospheres were characterized complementarily using XRD, HRTEM, XPS, and EDS. As illustrated in Figure S1, the XRD patterns demonstrated that the hollow Na_xWO_3 nanospheres are amorphous. This was verified independently by the HRTEM image (see Figure S2) on which there is no crystal lattice

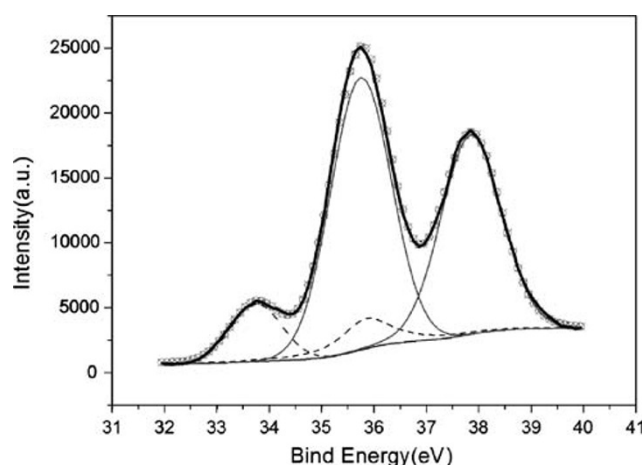


Fig. 2 XPS spectra of W ($4f_{7/2}$ and $4f_{5/2}$) in the hollow $\text{Na}_{0.15}\text{WO}_3$ nanospheres

observed. Figure 2 shows the XPS spectrum of W in the hollow Na_xWO_3 nanospheres. The two major W $4f_{7/2}$ and $4f_{5/2}$ peaks centered at 35.75 and 37.58 eV are assigned to the W^{6+} bound to oxygen. The corresponding binding energies of two relatively weaker W $4f_{7/2}$ and $4f_{5/2}$ peaks, 33.75 and 35.95 eV, are in agreement with the expected values for W^{5+} bound to oxygen [25]. The ratio of W^{5+} to W^{6+} estimated from the integrated areas of the aforementioned W 4f XPS peaks is about 0.18 [means $\text{W}^{5+}/(\text{W}^{5+} + \text{W}^{6+}) = 0.18/(0.18 + 1) \approx 0.15$]. This illustrates that the chemical formula of the hollow nanospheres should be $\text{Na}_{0.15}\text{WO}_3$. The EDS results acquired from the same hollow nanospheres were depicted in Figure S3. The as-determined Na content is of ~ 0.15 (atomic ratio to W), which is in full agreement with the XPS result.

Several mechanisms have been proposed for the formation of the nanosized hollow structures. The Kirkendall effect (simply be interpreted as an interfacial solid-state chemical reaction) has been widely used to explain the

formation of hollow structures via solid substance as the reactant as well as the “hard template” [3, 26, 27]. More recently, a gas–liquid interface aggregation mechanism was introduced to interpret the formation of hollow nanostructures with the gas bubble as a “soft template” [9]. The gas–liquid interface aggregation mechanism consists typically of three steps: the nanoparticle formation, diffusion, and aggregation. Differently, in our case, we believe that the hydrogen gas bubbles accumulated in the reaction system play dual roles: reducing chemically the tungstate to tungsten and guiding the formation of hollow $\text{Na}_{0.15}\text{WO}_3$ nanospheres. During the reaction, Na_2WO_4 was reduced to $\text{Na}_{0.15}\text{WO}_3$ at the interfaces of hydrogen gas bubbles and reaction solution, and the formed $\text{Na}_{0.15}\text{WO}_3$ condensed in situ at the interface forming the hollow structure. This is different from the aforementioned gas–liquid interface aggregation procedure, but more similar to Kirkendall effect. To confirm the indispensability of the hydrogen gas bubbles as templates for the formation of hollow structure, the temperature for Na_2WO_4 reduction with NaBH_4 was raised from 25 to 60, 80, and 100 °C while other reaction conditions were kept the same. Generally, high temperature accelerates the gas release from the reaction solution, thus would affect the amount of the hydrogen gas bubbles accumulated in the reaction solutions. As expected, the percentage of solid sodium tungsten bronzes nanoparticles in the product was increased with the increase in temperature. At 100 °C, only solid sodium tungsten bronzes nanoparticles were obtained as shown in Fig. 3. Additionally, during the course of the reaction, some hydrogen gas bubbles in the reaction solution unavoidably escaped from the solution before they were fully covered by $\text{Na}_{0.15}\text{WO}_3$, which results in the formation of the holes on the hollow shells, see Fig. 1a.

The metal oxide hollow nanoparticles, such as α - and γ - Fe_2O_3 , Fe_3O_4 , MnO_2 , and TiO_2 , have been used as adsorbents for removing the pollutants from water [1–4],

however, due to their reactions with acids, most of them cannot be stable in acidic water. Thus, the removal of pollutants from water using the metal oxides was usually performed under neutral or weak basic condition. Differently, the as-prepared $\text{Na}_{0.15}\text{WO}_3$ nanospheres are resistance to most acids. We found that after being immersed in water with $\text{pH} = 2$ for 2 days, the size and the hollow structure of the $\text{Na}_{0.15}\text{WO}_3$ nanospheres were still preserved well (Figure S5). Nitrogen adsorption isotherm showed that the BET specific area of hollow $\text{Na}_{0.15}\text{WO}_3$ nanospheres (Fig. 1) is $33.8 \text{ m}^2 \text{ g}^{-1}$, which is much larger than that ($9.3 \text{ m}^2 \text{ g}^{-1}$) of the same size solid $\text{Na}_{0.15}\text{WO}_3$ nanospheres (Fig. 3). The resistance to acids and large specific area of the as-obtained hollow $\text{Na}_{0.15}\text{WO}_3$ nanospheres suggest that the hollow $\text{Na}_{0.15}\text{WO}_3$ nanospheres might be an optimal adsorbent to remove organic pollutants from acidic waste water. To test this assumption, in a

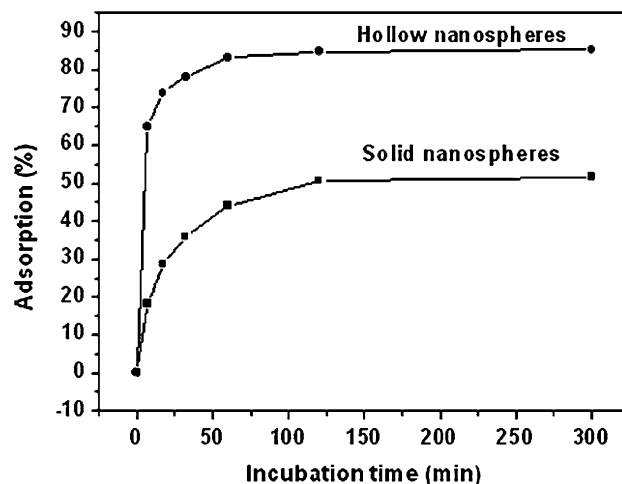


Fig. 4 Adsorption abilities of the hollow and solid $\text{Na}_{0.15}\text{WO}_3$ nanospheres to Coomassie Brilliant blue. Y axis is the percentage of Coomassie Brilliant blue adsorbed at the corresponding incubation time

Fig. 3 **a** FESEM and **b** TEM images of solid $\text{Na}_{0.15}\text{WO}_3$ nanospheres

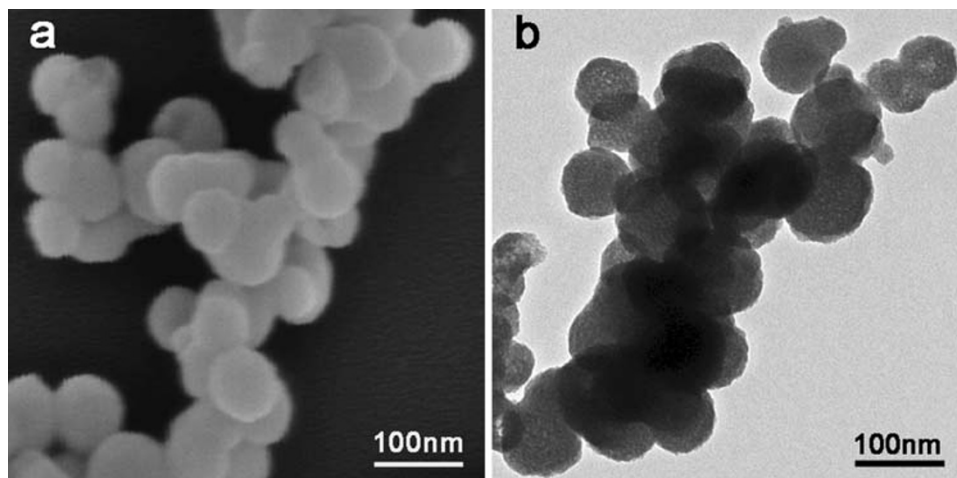
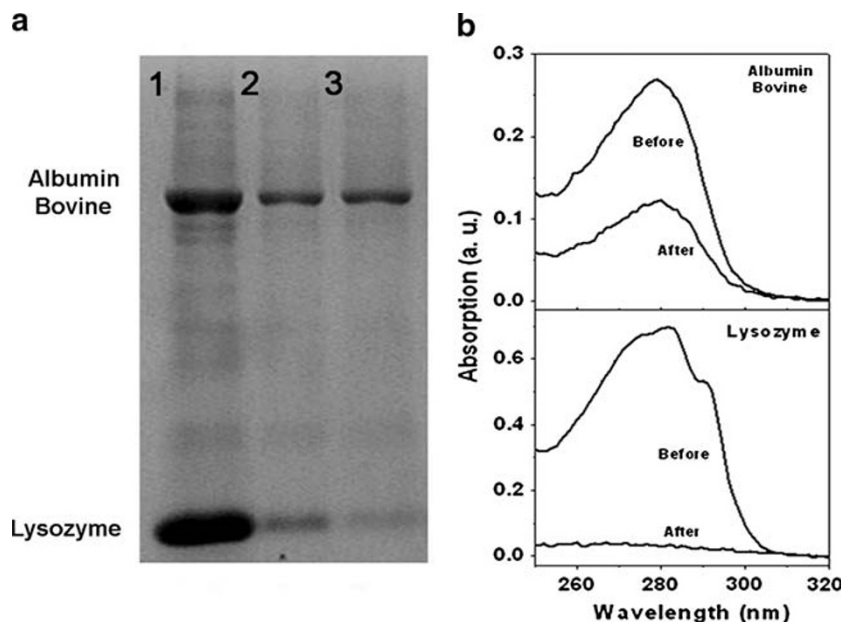


Fig. 5 **a** The image of gel electrophoresis of Albumin Bovine and Lysozyme. Lane 1, the mixture (1:3 in weight) of the two proteins; Lane 2 and 3, the mixture (1:3 in weight) of the two proteins after 5 min and 15 min incubation with hollow $\text{Na}_{0.15}\text{WO}_3$ nanospheres, respectively. **b** UV-vis spectra of Albumin Bovine and Lysozyme before and after incubation with hollow $\text{Na}_{0.15}\text{WO}_3$ nanospheres for 15 min



typical experiment, 100 mg of hollow $\text{Na}_{0.15}\text{WO}_3$ nanospheres was suspended in 2 mL, 60 $\mu\text{g}/\text{mL}$ of Coomassie Brilliant blue (a common dye) aqueous solution with $\text{pH} = 2$. The concentration variation of the Coomassie Brilliant blue in the supernatant as a function of adsorption time was followed using UV-vis spectroscopy. As shown in Fig. 4, 87% of the Coomassie brilliant blue was adsorbed within 300 min by the hollow $\text{Na}_{0.15}\text{WO}_3$ nanospheres at room temperature. For comparison, a similar experiment was performed with the solid sodium tungsten bronzes nanoparticles as adsorbent. As depicted in Fig. 4, after 300 min, only 50% of the Coomassie Brilliant blue was adsorbed by the solid sodium tungsten bronzes nanoparticles. Considering that the specific area of the hollow $\text{Na}_{0.15}\text{WO}_3$ nanospheres is almost three times of that of the solid $\text{Na}_{0.15}\text{WO}_3$ nanospheres, we, thus, believe that the surface absorption should play main roles for the removal of the dye molecules from water. In order to investigate the effects of pH value of waste water on the removal capacity of the hollow $\text{Na}_{0.15}\text{WO}_3$ nanospheres, the pH values of the Coomassie Brilliant blue aqueous solutions were varied from 1 to 6, but no obvious influences were observed.

Hollow $\text{Na}_{0.15}\text{WO}_3$ nanospheres could also be used to remove biomacromolecules from water. The adsorption abilities of the hollow $\text{Na}_{0.15}\text{WO}_3$ nanospheres to Albumin Bovine (MW, 66 kDa) and Lysozyme (MW, 14.3 kDa) were determined using gel electrophoresis and UV-vis spectroscopy. Figure 5a presents the images of sodium dodecyl sulfate polyacrylamide gel electrophoresis (SDS-PAGE) of mixture (Albumin Bovine to Lysozyme is 1:3 in weight) of two proteins before and after incubation with the hollow $\text{Na}_{0.15}\text{WO}_3$ nanospheres for 5 and 15 min, respectively. Lane 1 presents the as-mixed two proteins. Lane 2

and 3 show the supernatants after incubation with the hollow $\text{Na}_{0.15}\text{WO}_3$ nanospheres for 5 and 15 min, respectively. As seen from the intensities of the protein lanes, after 15 min adsorption, $\sim 50\%$ of Albumin Bovine and $\sim 95\%$ of Lysozyme were adsorbed. The protein concentration of each samples, before and after the adsorption, were also precisely determined using UV-vis spectroscopy. The results are shown in Fig. 5b. After 15 min incubation, 95% of Lysozyme was adsorbed, while only 50% of Albumin Bovine was adsorbed by the same amount of the hollow $\text{Na}_{0.15}\text{WO}_3$ nanospheres. This is consistent with the gel electrophoresis results. Such adsorption ability difference suggested that the large size protein could mainly be adsorbed on the outer surface of the hollow $\text{Na}_{0.15}\text{WO}_3$ nanospheres, while the small size protein might be adsorbed on both the outer and inner surfaces of the hollow nanospheres. Additionally, the different adsorption abilities to the proteins with different sizes could also be caused by the surface charge and structure difference of the proteins themselves. Nevertheless, the facts that Coomassie Brilliant blue and proteins with different sizes could be adsorbed by the hollow $\text{Na}_{0.15}\text{WO}_3$ nanospheres suggest that the hollow $\text{Na}_{0.15}\text{WO}_3$ nanospheres should be potentially useful in water treatment.

Conclusions

The hollow sodium tungsten bronze, $\text{Na}_{0.15}\text{WO}_3$, nanospheres have been successfully fabricated using the hydrogen gas bubbles as reactant to reduce the tungstate to tungsten and as template to direct the hollow structure formation as well. This, to our best knowledge, is the first

example of using hydrogen gas bubbles as reactant and template at the same time to prepare nanosized hollow materials, and should provide a general means for preparing other inorganic nanosized hollow materials. The resistance to most acids and the pronounced removal capacity of the as-synthesized hollow $\text{Na}_{0.15}\text{WO}_3$ nanospheres to small organic molecules and proteins from acidic waste water should find widespread applications in water treatment. Further studies on tailoring the surface chemistry and the shell porosity of the hollow $\text{Na}_{0.15}\text{WO}_3$ nanospheres would be essential to their practical applications and are under current investigation.

Acknowledgments This work was supported by the National Basic Research Program (973 program) of China (No. 2007CB936000), the National High Technology Research and Development Program (863 program) of China (No. 2006AA04Z309), and the Shanghai Pujiang Scholarship Program (Nos. 06PJ14025, 06PJ14030).

References

1. A.D. Dinsmore, M.F. Hsu, M.G. Nikolaides, M. Marquez, A.R. Bausch, D.A. Weitz, *Science* **298**, 1006 (2002)
2. J. Yuan, K. Laubernds, Q. Zhang, S.L. Suib, *J. Am. Chem. Soc.* **125**, 4966 (2003)
3. J. Fei, Y. Cui, X. Yan, W. Qi, Y. Yang, K. Wang, Q. He, J. Li, *Adv. Mater.* **20**, 452 (2008)
4. Y. Zhu, J. Shi, W. Shen, X. Dong, J. Feng, M. Ruan, Y. Li, *Angew. Chem. Int. Ed.* **44**, 5083 (2005)
5. F. Caruso, R.A. Caruso, H. Mohwald, *Science* **282**, 1111–1114 (1998)
6. J. Liu, D. Xue, *Adv. Mater.* **20**, 2622 (2008)
7. X.W. Lou, C. Yuan, L.A. Archer, *Adv. Mater.* **19**, 3328 (2007)
8. Q. Peng, Y. Dong, Y. Li, *Angew. Chem. Int. Ed.* **42**, 3027 (2003)
9. X. Wang, Q. Peng, Y. Li, *Acc. Chem. Res.* **40**, 635 (2007)
10. J. Huang, Y. Xie, B. Li, Y. Liu, Y. Qian, S. Zhang, *Adv. Mater.* **12**, 808 (2000)
11. S. Kim, M. Kim, W. Lee, T. Hyeon, *J. Am. Chem. Soc.* **124**, 7642 (2002)
12. Y. Ma, L. Qi, J. Ma, H. Cheng, W. Shen, *Langmuir* **19**, 9079 (2003)
13. E.O. Brimji, J.C. Brantey, H. Lorenaz, H. Jellinek, *J. Am. Chem. Soc.* **73**, 5427 (1951)
14. L.E. Conroy, *J. Chem. Educ.* **54**, 45 (1977)
15. B.A. Raby, C.V. Banks, *Anal. Chem.* **36**, 1106 (1964)
16. S. Raj, H. Matsui, S. Souma, T. Sato, T. Takahashi, A. Chakraborty, D.D. Sarma, P. Mahadevan, S. Osihi, W.H. McCarrroll, M. Geenblatt, *Phys. Rev. B Condens. Matter Mater. Phys.* **75**, 155116 (2007)
17. M.J. Sienko, S.M. Morehouse, *Inorg. Chem.* **2**, 485 (1963)
18. F.A. Cotton, G. Wilkinson, *Advanced inorganic chemistry*, 5th edn. (Wiley-Interscience, New York, 1988)
19. J. Wang, G. Liu, Y. Du, *Mater. Lett.* **57**, 3648 (2003)
20. R. Fan, X.H. Chen, Z. Gui, Z. Sun, S.Y. Li, Z.Y. Chen, *J. Phys. Chem. Solids* **61**, 2029 (2000)
21. A. Manthiram, A. Dananjay, Y.T. Zhu, *Chem. Mater.* **6**, 1601 (1994)
22. C. Tsang, S.Y. Lai, A. Manthiram, *Inorg. Chem.* **36**(/10), 2206 (1997)
23. G.K. Wertheim, M. Campagna, J.N. Chazalviel, H.R. Shanks, *Chem. Phys. Lett.* **44**, 50 (1976)
24. H.I. Schlesinger, H.C. Brown, A.E. Finholt, J.R. Gilbreath, H.R. Hoekstra, E.K. Hyde, *J. Am. Chem. Soc.* **75**(1), 215 (1953)
25. O.Y. Khyzhun, *J Alloy Compd* **305**, 1 (2000)
26. H.J. Fan, M. Knez, R. Scholz, K. Nielsch, E. Pippel, D. Hesse, M. Zacharias, U. Gosele, *Nat. Mater.* **5**, 627 (2006)
27. A.D. Smigelskas, E.O. Kirkendall, *Trans. Am. Inst. Min. Metall. Pet. Eng.* **171**, 130 (1947)